

UNCLASSIFIED

Defense Technical Information Center  
Compilation Part Notice

ADP012611

TITLE: Depth Profiling of SiC Lattice Damage Using Micro-Raman Spectroscopy

DISTRIBUTION: Approved for public release, distribution unlimited

This paper is part of the following report:

TITLE: Progress in Semiconductor Materials for Optoelectronic Applications Symposium held in Boston, Massachusetts on November 26-29, 2001.

To order the complete compilation report, use: ADA405047

The component part is provided here to allow users access to individually authored sections of proceedings, annals, symposia, etc. However, the component should be considered within the context of the overall compilation report and not as a stand-alone technical report.

The following component part numbers comprise the compilation report:  
ADP012585 thru ADP012685

UNCLASSIFIED

### Depth Profiling of SiC Lattice Damage Using Micro-Raman Spectroscopy

Iulia C. Muntele, Daryush Ila, Claudiu I. Muntele, David B. Poker<sup>1</sup>, Dale K. Hensley<sup>1</sup>  
Center for Irradiation of Materials, Alabama A&M University, Normal, AL – 35762, U. S. A.  
<sup>1</sup>Solid State Division, Oak Ridge National Laboratory, Oak Ridge, TN, U. S. A.

#### ABSTRACT

Depth profiling for the amount of lattice damage using a Confocal Micro-Raman (CMR) spectrometer is demonstrated in this paper. Samples of n-type silicon carbide were implanted with 2 MeV He and O ions at both room temperature and 500 °C, and fluences between  $10^{15}$  and  $10^{17}$  ions/cm<sup>2</sup>. Post-implantation annealing at 1000 °C was also performed in order to study the damage evolution. Optical Absorption Spectrophotometry (OAS) was used for establishing the opacity (and therefore the probing depth) of the damaged layer to the 632.8 nm wavelength of the He-Ne laser used for CMR throughout this study. The methodology used and the results obtained are presented herein. Total dissipation of amorphous carbon islands was observed even at low annealing temperatures of the RT implanted samples, along with an increase in the size of the amorphous silicon islands.

#### INTRODUCTION

In device fabrication the ion implantation is usually the doping method of choice because it offers precise control over the spatial distribution and doping level using conventional masking techniques. Hot implantation of silicon carbide is a common practice aimed at reducing the damages incurred during the passage of ions through the material, reducing the needs for post-implantation annealing for crystalline lattice recovery. Although literature mentions that strong dynamical recovery has been achieved at temperatures as low as 200 °C, an annealing temperature up to 1700 °C is still necessary for an acceptable degree of lattice recovery, especially for Al-doped p-type silicon carbide. In order to predict a certain type of behavior of an electronic device, it is important to know the depth distribution of the residual damage present in the crystalline lattice. This is necessary because the carrier trapping levels introduced in the band gap by lattice damages (vacancies, interstitials, substitutionals etc.) can significantly change the electric behavior. Techniques like Positron Annihilation Spectroscopy [5,6] and Rutherford Backscattering/Channeling Spectrometry [7] have been reported in the literature as good tools for this type of investigation. This paper is intended to present an all-optical approach of this problem, using a CMR spectrometer for depth monitoring of the 400 – 600 cm<sup>-1</sup> (amorphous silicon) and 1250 – 1450 cm<sup>-1</sup> (amorphous carbon) spectral regions. Also, an UV/Vis (200 – 980 nm wavelength range) spectrophotometer was used for optical absorption measurements aimed at establishing the probing depth of the He-Ne laser (632.8 nm wavelength) used by the CMR spectrometer. The SRIM computer code was used as well, for establishing the ranges of the He and O ions into silicon carbide, and to provide a depth profile for the number of displaced atoms from the silicon carbide crystalline lattice during the implantation process.

## METHODOLOGY FOR ANALYSIS

The confocal sampling mode of the micro Raman spectrometer [1] introduces the advantage of reduced/controlled depth of focus, resulting in an increased resolution on the z-axis (the normal at the surface of the sample). Experimentally, the confocality is measured usually by plotting the intensity of the only Raman line of silicon ( $520 \text{ cm}^{-1}$ ) as a function of the position of the focus on the z-axis. The curve obtained for a confocal hole of  $200 \mu\text{m}$  has an almost gaussian shape, with the second order momentum (the square root of the variance) equal to:

$$\sigma = \frac{n\lambda}{4 \cdot NA^2} \quad (1)$$

For n-type 6H silicon carbide, considering  $n=2.66$  (the refractive index),  $\lambda=632.8 \text{ nm}$  (the wavelength of the He-Ne laser), and the numerical aperture of the objective  $NA=0.9$  (for the 100X objective), this quantity is  $520 \text{ nm}$ . Therefore, the FWHM (full width at half maximum = the measure for confocality) of the Raman intensity curve becomes  $1.22 \mu\text{m}$  ( $\text{FWHM} = 2.35 \times \sigma$ ). This value is associated with the diameter of the spot in the sample where the laser beam is focused, and from where the Raman signal is collected. However, in implanted silicon carbide samples, the photoabsorption coefficient of the material increases to very high values, absorbing the probing light into a much lesser distance than the one given by the confocality. Therefore a "probing depth" for a particular combination target - laser beam is introduced [2] as:

$$d_p = -\frac{1}{2\mu} \ln \left( \frac{I_d}{I_s + I_d} \right) = \frac{2.3}{2\mu} \quad (2)$$

with  $I_s$  the intensity of the light scattered from the surface of the sample to the depth  $d_p$ ,  $I_d$  the intensity of the light scattered from the depth  $d_p$  to infinity, and  $\mu$  the photoabsorption coefficient. The number in the second part of the formula above (2.3) appears when a generally accepted 0.1 value for the ratio between the  $I_d$  and the total scattered light is considered. One can see that extrapolating for an infinite high photoabsorption coefficient (opacity of the sample), the probing depth goes to zero, and thus having analyzed only the surface of the sample.

UV/Vis Optical Absorption Spectrophotometry (OAS) was used for determining the photoabsorption coefficient of the layer damaged by ion implantation. The absorbance  $A$  measured in OAS is related to this coefficient by:

$$A = \lg(e^{\mu d}) = k\mu d \quad (3)$$

with  $k = 0.4343$  and  $d$  the distance traveled by the electromagnetic radiation through the material of photoabsorption coefficient  $\mu$  [8]. Assuming a constant coefficient  $\mu'$  for the implanted layer of thickness  $d'$ , one can calculate it from:

$$\mu' = \mu + \frac{A' - A}{kd'} \quad (4)$$

The value for  $d'$  can be easily estimated from damage distributions given by SRIM simulations for the ion implantation process, and the two absorbances (for the sample after and before implantation, at the wavelength of the laser beam used in CMR) can be obtained from OAS.

## EXPERIMENT AND RESULTS

Samples of n-type (N-doped) silicon carbide were implanted with helium and oxygen at 2 MeV and fluences between  $10^{15}$  and  $10^{17}$  ions/cm<sup>2</sup> at both room temperature (RT) and 500 °C. The ion implantation was carried out at the Oak Ridge National Laboratory. Table I presents the implantation conditions for the samples used in this study. The post-implantation annealing in argon at 500 and 1000 °C, and the optical analysis were performed at the Center for Irradiation of Materials of Alabama A&M University. Optical measurements (OAS and CMR) were employed before implantation and after each annealing step. Unimplanted silicon carbide samples were also annealed in identical conditions, for monitoring the original defect evolution, as a baseline for the defect densities of the implanted samples. The parameters used for the CMR spectrometer were 200  $\mu$ m confocal hole, 100X objective, 1800 g/mm grating, 20 mW He-Ne laser ( $\lambda=632.817$  nm), and a Peltier cooled CCD detector. The spectra were acquired in the 300-700 cm<sup>-1</sup> region for amorphous silicon and Si-Si characteristic peaks and 1200-1700 cm<sup>-1</sup> region for amorphous carbon. OAS was performed in the 200-980 nm wavelength range, although only absorbance values at 632.8 nm were of interest for this work.

The depth scanning was performed with a 1  $\mu$ m step, starting at the surface of the sample and ending after the entire range of the implanting ions was covered, when possible (probing depth large enough). The ion ranges were obtained from SRIM. Figure 1 presents the damage profiles taken for both amorphous silicon and amorphous carbon regions for the as implanted samples. Only for two samples was possible a depth profiling, the others being opaque for 632.8 nm wavelength of the laser, therefore having Raman signal collected just from the surface. Figure 2 presents data for the RT implanted samples after annealing for 1 hour at 500 °C in argon, compared to the samples implanted at 500 °C to see the difference made by the hot implantation vs. cold implantation + annealing. Figure 3 presents the damage profiles of the samples after annealing for 1 hour at 1000 °C in argon. Damage profiling on unimplanted silicon carbide annealed in the same conditions as the implanted samples was also carried out and the results are presented in Figure 4, only for the amorphous silicon region.

**Table I.** Implantation parameters for the silicon carbide samples used in this work.

Parameter	Sample number							
	46	48	49	50	55	56	59	60
Ion	He	He	He	He	O	O	O	O
Energy (MeV)	2	2	2	2	2	2	2	2
Fluence (cm <sup>-2</sup> )	$10^{15}$	$10^{17}$	$10^{15}$	$10^{16}$	$10^{15}$	$10^{17}$	$10^{15}$	$10^{16}$
Implantation Temperature	RT	RT	500 °C	500 °C	RT	RT	500 °C	500 °C

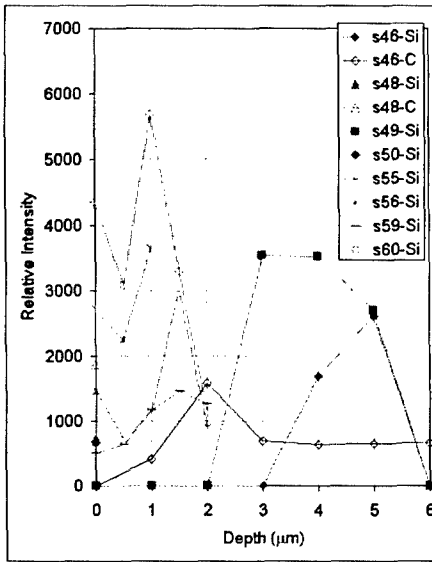


**Figure 1.** RT vs. 500 °C ion implantation.

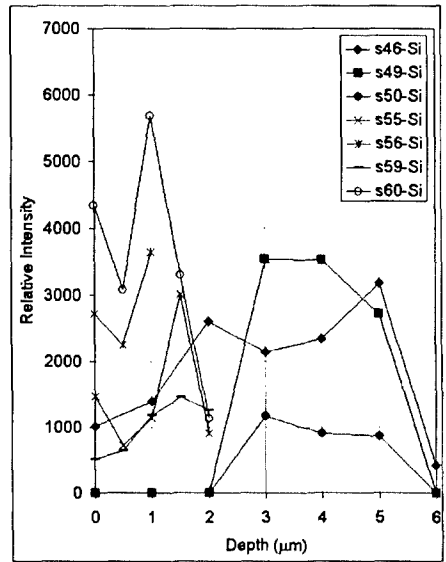


**Figure 2.** Implantation + annealing vs. hot implantation (all at 500 °C).

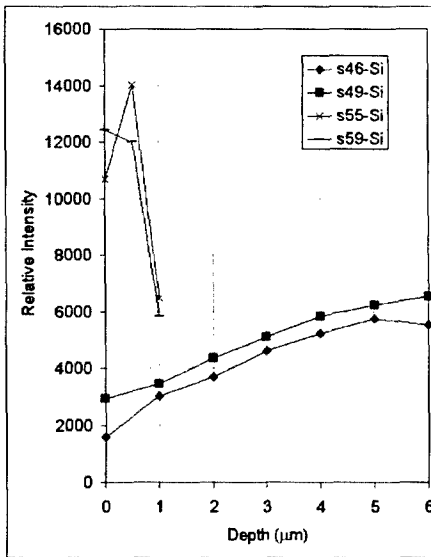


**Figure 3.** After annealing at 1000 °C. only).

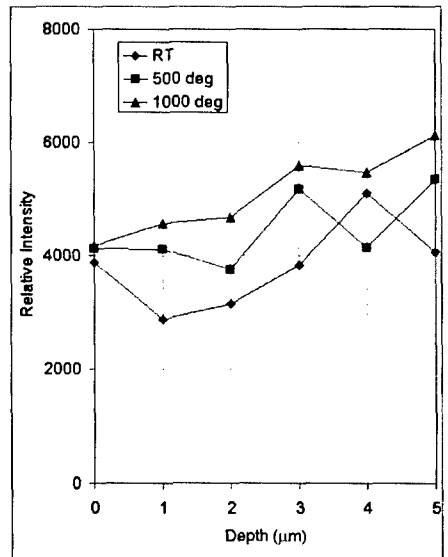


**Figure 4.** Pristine SiC (Si profiling

## DISCUSSIONS

From Figure 1 one can see that the depth profiling was possible only for a few samples. The "Si" or "C" symbols in the legend show for which amorphous region is the respective plot taken. The plots monitoring the silicon region follow a shape mimicking the distributions given by SRIM simulations for silicon displacements, with maximum values at the depth where the helium and oxygen ions stopped in the material (4.66 and 1.6  $\mu\text{m}$ , respectively). This is an unsurprising result, knowing that the damage is caused by the nuclear energy loss, which is the dominating process toward the end of the ion's range. What is surprising is that the amount of damage is greater in case of hot implantation than the RT implantation, leading to the conclusion that silicon is easier to be displaced at higher temperatures, and the damaged crystalline lattice is not recovering from this, as in the general case of other semiconductors. However, there is no amorphous carbon to be monitored for the sample that was hot-implanted, whereas for the sample implanted at RT there is a relatively massive amorphization of carbon present, with an almost uniform distribution in depth, during the entire range of helium ions. Since the sample implanted at 500 °C is more transparent to visible light than the one implanted at RT, one can conclude that the cause for losing the transparency is the amorphous carbon islands created during implantations. Post-implantation annealing to 500 °C of the samples implanted at RT (see Figure 2) presented a better transparency to visible light, allowing the depth profiling for most of the samples, also correlated to the complete disappearance of the amorphous carbon peak. However, instead of approaching the amorphous silicon distributions for the hot-implanted samples, the silicon amorphization region in sample 46 increases and spreads within the sample, showing that the situation actually worsens for the crystalline lattice. This situation is confirmed in Figure 3, where the distributions for all the samples presented there show an overall increase by a factor of 2, along with a "leveling" (more significant in the case of helium implanted samples). Also, the difference between the samples implanted at RT and the ones hot-implanted becomes negligible at this point. The confirmation that this is an effect due solely to the ion implantation, Figure 4 shows the non-implanted witness sample, whose amorphous silicon distribution remains relatively unchanged throughout the temperature range investigated.

## CONCLUSIONS

The work presented here demonstrates that is possible to use a CMR setup for monitoring the depth distribution of damages in materials that are relatively transparent to the wavelength of the laser used. A methodology for estimating the depth resolution is described, and the techniques for obtaining the parameters involved are mentioned.

It has been shown that hot-implantation of silicon carbide is preferable over RT implantation followed by annealing. In addition, it was shown a complete dissipation of the amorphous carbon regions even at low annealing temperatures. As for the amorphous silicon regions in the material, it was shown that they do not dissipate, but rather increase in dimensions with the annealing temperatures. Further studies at higher temperatures are recommended for future work, for an accurate monitoring of their evolution.

## ACKNOWLEDGEMENTS

This work is supported by the Center for Irradiation of Materials at Alabama A&M University and NASA-GRC Contract No. NAG3-2123. The work at ORNL was sponsored by the U.S. Department of Energy under contract DE-AC05-01OR22725 with the Oak Ridge National Laboratory, managed by UT-Battelle, LLC.

## REFERENCES

1. Labram User Manual, ISA Dilor-Jobin Yvon, 1999.
2. "Raman and Luminiscence Spectroscopy for Microelectronics", Catalogue of Optical and Physical Parameters, "Nostradamus" Project SMT4-CT-95-2024, European Commission, 1998.
3. The Stopping and Ranges of Ions in Solids, J. F. Ziegler, J. P. Biersack, U. Littmark, Pergamon Press, 1985.
4. N. B. Colthup, L. H. Daly, S. E. Wiberley, "Introduction to Infrared and Raman Spectroscopy", Third Edition, Academic Press, 1990.
5. Y. Tanaka, N. Kobayashi, H. Okumura, R. Suzuki, T. Ohdaira, M. Hasegawa, M. Ogura, S. Yoshida, H. Tanoue, "Electrical and Structural Properties of Al and B Implanted 4H-SiC", Materials Science Forum Vols. 338-342 (2000), Trans Tech Publications, pp. 909-912.
6. W. Puff, A. G. Balogh, P. Mascher, "Microstructural Evolution of Radiation-Induced Defects in Semi-Insulating SiC During Isochronal Annealing", Materials Science Forum Vols. 338-342 (2000), Trans Tech Publications, pp. 965-968.
7. Handbook of Modern Ion Beam Materials Analysis, Material Research Society, 1995, Chapter 10, pp. 231-300.
8. P. D. Townsend, P. J. Chandler, L. Zhang, "Optical Effects of Ion Implantation", Cambridge University Press, 1994, pp. 71-72.